Applications of High-Resolution Optical Spectroscopy in Optical Networks Research

(Invited)

I. Garcés, A. Villafranca, J.J. Martínez, J. Lasobras, A. López and M.A. Losada

[2] Photonics Technology Group, I3A, University of Zaragoza, Zaragoza, Spain
Tel: +34 976 761964, Fax: +34 976 762111, E-mail: ngarces@unizar.es

High-resolution optical spectroscopy (HROS) is emerging as a novel and promising measurement technique to study optical signals with applications into multiple research fields. In this communication, the key aspects for HROS for its use as a measurement and characterization technique in the field of optical networks research will be addressed. Considered applications include the characterization of dynamic parameters of optical sources, the proposal of new bandwidth effective frequency modulation formats with application to labeling and WDM-PONs, and the study of Brillouin and Rayleigh scattering effects in single-fibre remote feeding architectures.

1. Introduction

The optical intensity spectrum of a signal contains very significant information, but extracting it is a very hard task, as most of the technologies used for these means have limitations either in the frequency resolution, or in the dynamic range of the power measurement, or fail in achieving a good compromise between both restrictions. But even with these limitations, optical spectrum analyzers based on diffraction gratings, with resolutions in the order of tens of picometers have proven to be very useful both for laboratory purposes and for network measurements, while the higher resolution obtained with interferometric devices such as Fabry-Perot interferometers is also useful for some characterizations despite its lack of dynamic range, so there is no doubt that the information contained in the optical spectrum of a signal is relevant and efforts put into measuring it are worthy.

High-resolution optical spectroscopy (HROS) is emerging as a new measurement technique to study optical signals with applications into multiple research fields. Optical communication signals transmitted through optical networks enclose important information that is not easily obtained using standard techniques. We have used a new HROS technology based on Stimulated Brillouin Scattering (SBS) effect [1] in optical fibres to analyse optical signals related to optical networks, including the characterization of dynamic parameters of optical sources [2] (Directly Modulated Lasers, Integrated Laser Modulators), the proposal of new bandwidth effective frequency modulation formats with application to labelling and WDM-PONs [3], and the study of Brillouin and Rayleigh scattering effects in single-fibre remote feeding architectures [4]. A new technique based on the same SBS technology to obtain the phase of modulated optical signals has also been developed and tested [5].

The equipment used to perform these measurement techniques is called BOSA and has been developed by Aragon Photonics Labs. in collaboration with the Photonics Technology Group of University of Zaragoza. This analyzer has some interesting properties, associated to the properties of the Brillouin scattering and to the fact that the processing is performed in the optical domain, which makes the measurement process very fast. With the BOSA, an analysis filter of 0.08 pm, or 10 MHz, bandwidth is used to scan the wavelength region of interest. This filter has a Gaussian profile, that makes it steeper than other techniques used for spectral analysis, and thus it obtains a higher optical rejection ratio (±45 MHz @ 40 dB) and a higher dynamic range of around 80 dB.

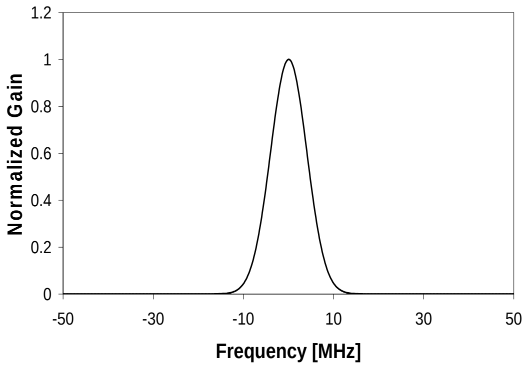

Figure 1: Normalized filter frequency response of the BOSA

Measuring the optical spectrum with this scope reveals details that cannot be measured by other means, as are normally not resolved either in frequency or in power. The measurements performed here are the closest to the “ideal” optical spectrum with theoretical infinite resolution to our knowledge. However, the optical spectrum we present are well known from literature and optical communications simulators, so there is a lot of information about them and thus a very precise analysis of the measurement can be made. In next sections we will focus in the applications where we used HROS to obtain relevant information of the spectrum of optical signals related to optical networks research.

2. Optical source characterization

The CW spectrum of a semiconductor laser contains all the information needed to characterize its work parameters, but is not normally not exploited because measuring it with enough resolution or dynamic range, and specially with a good combination of both, is hard with traditional optical spectrum analyzers (OSA) based on gratings and other spectrometry techniques such as tunable Fabry-Perot filtering or heterodyne detection.

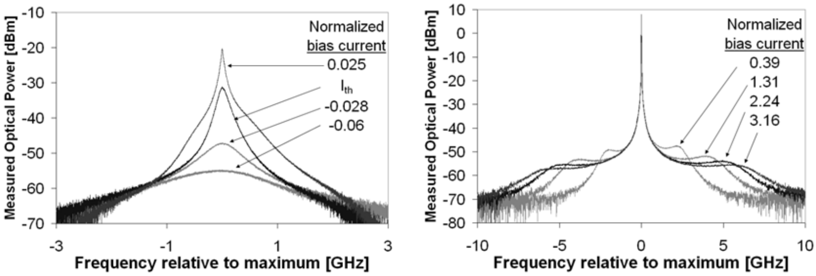

Figure 2: CW optical specrum of a DFB laser at several biasing currents around threshold (left) and far over threshold (right). Bias current is normalized: $I_{bias}/I_{th}-1$

In figure 2 the spectra of a DFB semiconductor laser operated in CW is shown. The lower curves on the left correspond to spontaneous emission below threshold and they have a typical Gaussian lineshape, with a width in the order of the GHz. As bias current is increased, stimulated emission becomes dominant and the width of the spectrum decreases, especially when approximating to the threshold current. Also the lineshape suffers some changes, resulting in a very well fitted Lorentzian function around threshold. At this point, only the phase noise of the laser is considered.

If we continue rising the bias current, an additional phenomenon can be observed as a certain deformation in the Lorentzian shape of the spectrum, as can be seen in the curves shown in figure 2 (right). The laser intensity noise appears as a soft increase of the power spectral density at frequencies far from the peak of power where the spectral density due to phase noise has fallen to very low values. The sum of phase noise and intensity noise forms a certain plateau that continues until a maximum is reached and then decreases sharply.

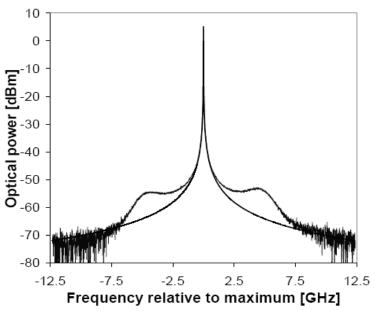

Figure 3: Lorentzian fitting to the spectral lineshape of a DFB laser. Laser intensity noise produces the additional spectral density.

A fitting of the measured optical spectrum to a Lorentzian function is shown Fig. 3. Linewidth values can be obtained from this fitting. The remaining power spectral density after subtracting this profile is basically the intensity noise spectrum, which can be used to calculate both the relaxation oscillation peak frequency and the RIN. Using linewidth values, the linewidth enhancement factor or alpha factor, can also be obtained.

TABLE I

Parameter		Laser DFB
I_{th}	mA	21.55
P_{out}	mW	1.95
SE	W/A	0.08
λ_p	nm	1543.64
α		3.6
RIN	dB/Hz	-125.67
f_R	GHz	3.64
γ_R	GHz	0.87

I_{th} – threshold current; P_{out} – emitted power; SE – Slope efficiency in linear regime; λ_p – peak wavelength; α – Linewidth enhancement factor; RIN – Relative intensity noise; f_R – relaxation oscillations peak frequency. All measurements are performed at 25º C. P_{out}, λ_p, α, RIN, f_R and γ_R are given at $I_{bias}=2 \cdot I_{th}$

Table I shows most of the parameters that can be obtained using HROS over CW emitting lasers, and measured values for the DFB laser whose spectra are shown in figure 2. This method has also been applied to MQW-DFB and VCSEL lasers, and results can be found in [2].

One parameter that has not been listed in Table I is the adiabatic chirp parameter found in standard directly modulated lasers. This parameter is of less importance for high bit rate sources, but can be used, as will be shown below, for obtaining frequency modulation at lower bit rates.

3. Narrow-FSK packet labeling

To accomplish an efficient routing in optical packet networks the labeling information must be inserted into packets or bursts. One of these labeling techniques is orthogonal labeling where two independent modulation dimensions are used for payload and label. Our proposal uses the adiabatic chirp of a DFB laser induced by a very low modulation depth to achieve a narrow-FSK separation between ‘1’ and ‘0’ levels. Label information will be present in this modulation while payload information is applied over the resulting signal by intensity modulation (IM) of the optical source.

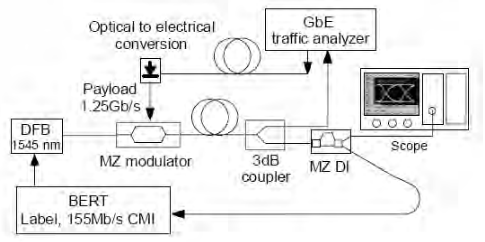

Figure 4: Experimental scheme for perform optical labeling of GbE frames.

Figure 4 depicts the experimental setup used in our labeling experiment. Our laser source was a 1545 nm DFB (adiabatic chirp 3 GHz/mW), and labels were introduced using a 155 Mb/s electrical signal of 3 mA peak-to-peak superposed over laser's bias and generated by a data communications BERT. Gigabit Ethernet frames used as payload information were generated by a GbE analyzer and utilized to drive a Mach-Zehnder Modulator (MZM) that applied IM on source signal. Narrow-FSK signal shows an optical frequency deviation between peaks in the range of a GHz (figure 5). The extraction of the label at the reception end was performed by a custom MZI filter specifically designed for this separation; it discriminates one of the FSK peaks, transforming the frequency modulation into an amplitude modulation and allowing us to carry out normal detection on the received signal.

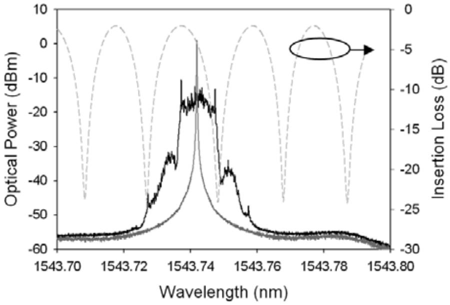

Figure 5: Spectra of CW signal and GbE FSK modulated signal; demodulator filter response.

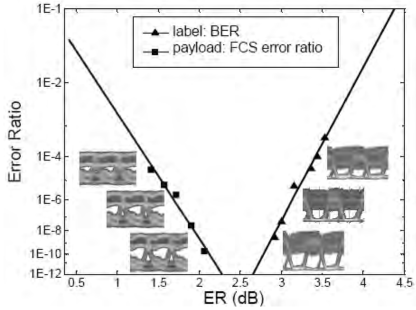

Figure 6: Payload and label performance for different payload's ERs with transmitted signal eyes. Optimal values are within the error-free region between the two lines.

A critical factor of the labeling system resides in the fact FSK modulation generates a residual IM that can interfere with the payload data, in this scenario there are two factors that must be precisely adjusted: One is FSK frequency separation that depends on the modulation depth and on the adiabatic chirp characteristics of the laser, it must be tuned to fit the demodulation filter and to minimize the residual IM modulation; The second is the MZM operation point that changes payload extinction ratio (ER): high ER leads to better payload detection but it degrades label transmission so payload and label performance have a trade-off in terms of payload ER. Both parameters can be better studied and adjusted applying HROS, figure 6 portrays the compromise in ER election, showing that optimal value is near 2.5 dB.

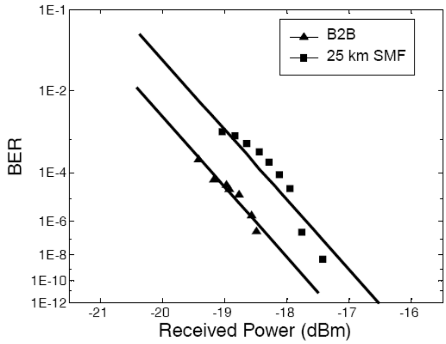

Figure 7: Label transmission performance: back-to-back and with 25 km SMF.

BER for the label at the reception end is represented in figure 7 for a back-to-back configuration and over 25 km SMF. Power penalty introduced by fiber is 0.85 dB, demonstrating the robustness of labeling method. Payload was even more tolerant to errors, achieving distances up to 50 km with error free behavior.

4. IM-FSK scheme in WDM-PON architecture

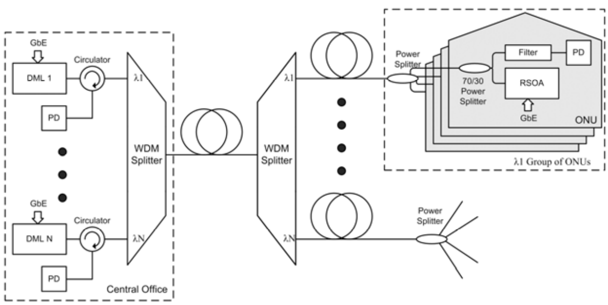

Figure 8: WDM-PON network architecture.

A similar narrow-FSK/IM modulation scheme has been applied in WDM-PON networks like to one show in figure 8, where central office (CO) has a set of directly modulated DFB lasers, each one serving different groups of users. By direct modulation of each wavelength source narrow-FSK modulation is applied at downstream transmission, the same laser source is used to feed the end user to perform upstream transmission via IM (optical loop-back). This lead to two advantages: first one is using the same ONU design for all users because it's independent for the wavelength, reducing costs and complexity; second is the flexibility of having an unique wavelength for both ways of communication, allowing a great increment of the number of users in already deployed PONS without any infrastructure modification.

In WDM-PON transmissions the ER of the signal is not a key issue, since the different modulation schemes are never applied to the optical source at the same time, so intensity modulation can be applied at better possible ER because there is no need anymore to recover FSK data. This fact makes the calibration of the different components far easier than in the case of FSK-labeling.

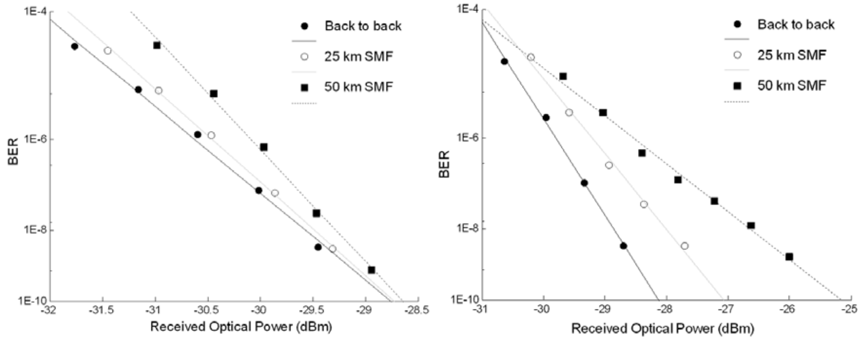

Figure 9: BER curves for downstream (a) and upstream (b) links, at back to back, 25 km SMF and 50 km SMF.

Figure 9 shows BER performance of the links in the experiment. In downstream link (a) we can see that the power penalty associated with fiber chromatic dispersion is negligible at 25 km and only slightly higher at 50 km, which shows that chromatic dispersion is not a critical factor as a result of the small spectral width of the narrow-FSK modulated signal. For upstream transmission (b) we can clearly see that dispersion have a more negative effect than in FSK transmission, although power penalty for 50 km of SMF is still low (about 2.5 dB), this degradation can be explained by the joint effects of the ASE to signal ratio in the fiber and the reflections of the RSOA output optical power. Even with these small penalties, both channels have a very high power budget working with 50 km of SMF, which confirms the viability of this scheme for its use in WDM-PON networks.

5. Backscattering in remote seeded networks architectures

In the previously proposed PON architecture the upstream link can experiment degradation caused by the backscattering effects arising at the SMR fibre due to the high injection power required to feed the remote users. Two main backscattering effects appear in our system: Rayleigh Scattering (RS), placed at the same wavelength than the original source signal and Brillouin Scattering (BS) which peak in our scheme with 25 km of SMF is placed about 11 GHz from the source wavelength. The RS peak has been thoughtfully studied in this environment because it’s located right inside the upstream signal; it has been proved that its effects can degrade the transmitted data. BS has not been studied so extensively because the back-scattered peak is outside upstream wavelength, however, BS power can be very high in these situations, affecting upstream transmission. With the use of HROS it’s possible to clearly measure the levels of RS and BS in a single fibre PON under diverse conditions such as different injected source powers and different spectral broadenings (obtained by direct modulation of the laser); and how this phenomena affect an upstream transmission. Figure 10 shows the backscattered signals measured at upstream link’s reception end; spectra for different injected powers without source modulation can be seen in figure 10 a), it’s clear that an increase in the injected optical powers rises both RS and BS, although Brillouin’s increase is far greater than Rayleigh’s.

Figure 10 b) shows the effects of applying a direct modulation to the bias laser in order to spread the source’s spectrum (narrow-FSK), the result is that RS power hardly changes while BS power is visibly mitigated. Total backscattered power can be appreciated in figure 11: the previous seen behaviour of BS and RS with the increasing input optical power is noticeably shown; also, increasing narrow-FSK modulation levels (no modulation, 1.5 mApp and 2.5 mApp over bias) lowers BS rising speed (initial and final levels are close in the three cases) while letting RS unaffected.

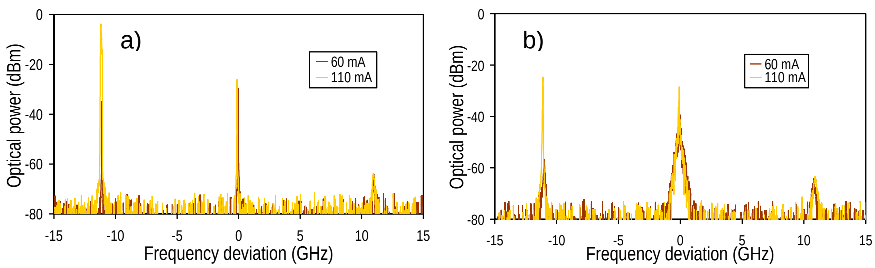

Figure 10: Spectra for different injected source powers, a) without source broadening, b) with narrow-FSK source broadening

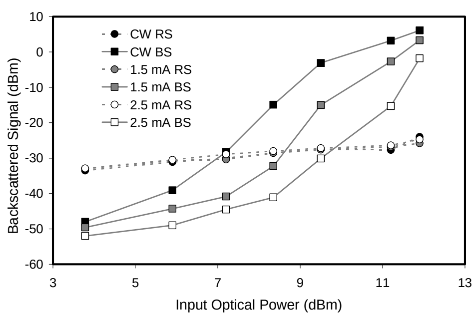

Figure 11: Total detected backscattered power for variable injected power, at different broadenings.

Acknowledgements

This work was supported in part by the funding of the Diputacion General de Aragon for I3A laboratories at Walqa Technology Park and Cátedra Telefonica.

References

[1] J. Subias, J. Pelayo, F. Villuendas, C. Heras, and E. Pellejer, “Very High Resolution Optical Spectrometry by Stimulated Brillouin Scattering,” *IEEE Photonics Technology Letters*, vol. 17, no. 4, pp. 855–857, 2005.

[2] A. Villafranca, J. Lasobras, J. A. Lazaro, and I. Garces, “Characterization of the main semiconductor laser static and dynamic working parameters from CW optical spectrum measurements,” *IEEE Journal of Quantum Electronics*, vol. 43, no. 2, pp. 116–122, 2007.

[3] I. Garcés, J. Aguado, J. Martínez, A. López, A. Villafranca, and M. A. Losada, “Analysis of narrow-FSK downstream modulation in colourless WDM PONs,” *Electronics Letters*, vol. 43, p. 471, 2007.

[4] J. J. Martinez, I. Garces, A. Lopez, A. Villafranca, J. C. Aguado, and M. A. Losada, “Novel WDM-PON architecture based on a spectrally efficient IM-FSK scheme using DMLs and RSOAs,” *Journal of Lightwave Technology*, vol. 26, pp. 350–356, Feb. 2008.

[5] A. Villafranca, J. Lasobras, R. Escorihuela, R. Alonso, and I. Garcés, “Time-resolved chirp measurement using complex spectrum analysis based on stimulated Brillouin scattering,” *Proceedings of OFC,* paper OWD4, Feb. 2008.